

Hyperpolarized ^{129}Xe Imaging of the Lung using Spiral IDEAL

Ozkan Doganay^{1,2}, Trevor Wade², Elaine Hegarty², Krzysztof Wawrzyn², Rolf F. Schulte³, Charles McKenzie^{1,2}, and Giles Santyr^{2,4}

¹Western University, London, Ontario, Canada, ²Robarts Research Institute, London, Ontario, Canada, ³GE Global Research, Munich, Germany, ⁴Peter Gilgan Centre for Research and Learning, Toronto, Ontario, Canada

Introduction: MRI of hyperpolarized (Hp) ^{129}Xe promises to provide unique functional information for diagnosis of lung disease, including ventilation, perfusion and gas exchange. Although most of the inhaled Hp ^{129}Xe remains in the gas phase, approximately 2% dissolves in the pulmonary tissue and red blood cell (RBC) compartments and these can be spectrally resolved using Dixon-based methods, taking advantage of the unique chemical shifts of ^{129}Xe dissolved in tissue (197 ppm) and RBC (217 ppm) compartments respectively. In particular, the IDEAL (Iterative Decomposition of water and fat with Echo Asymmetry and Least-square estimation) approach has been shown to be an efficient technique to image gas, tissue and RBC phases simultaneously [1, 2]. It is also anticipated that Hp ^{129}Xe imaging will benefit from single-shot acquisitions (eg. spiral), that cover k-space following a single excitation pulse, thereby making efficient use of the non-renewable Hp magnetization compared to Cartesian read-out approaches [3]. In this study, we implemented a spiral IDEAL approach for imaging dissolved Hp ^{129}Xe . The expected spatial resolution and SNR with respect to the readout time, T_{readout} , were calculated from the point spread function (PSF) and optimized for *in vitro* and *in vivo* imaging based on measured T_2^* values. The spiral approach was tested experimentally in a gas/dissolved Hp ^{129}Xe phantom and *in vivo* in rat lungs.

Methods:

Theory: The PSF for both Cartesian and the spiral k-space trajectories were calculated as a function of $T_{\text{readout}} / T_2^*$ as described previously [2] and the spatial resolution was estimated from the full width half maximum (FWHM) of the PSF. A normalized SNR, SNR_N , was calculated from the corresponding PSF amplitude, $A(T_{\text{readout}} / T_2^*)$, for a constant bandwidth and resolution using the following expression:

$$\text{SNR}_N \propto A(T_{\text{readout}} / T_2^*) \times \sqrt{N_r(T_{\text{readout}})} \times \sin \alpha$$

excitation pulses [6]. Theoretical maximum gradient amplitude (G_{max}), and slew rate, (SR) were then calculated for spiral trajectories corresponding to: $T_{\text{readout}} / T_2^* = 0.5, 1, 1.7, \text{ and } 3.2$. Spiral gradient waveforms (G_x, G_y) and k-space trajectories were then designed separately for phantom and *in vivo* imaging based on measured T_2^* values [4] as described below.

Experimental: All experiments were conducted using a 3T MRI system (MR750 GEHC, GE, Wisconsin, USA) and a custom built transmit-only/receive-only birdcage coil [5] and high performance insertable gradient system. A phantom consisting of a 125mL plastic bottle filled with 65mL water and 60mL Hp ^{129}Xe (natural abundance, polarization of ~5%) was used to confirm the theoretical SNR and spatial resolution *in vitro*. For *in vivo* testing, healthy Sprague Dawley rats were ventilated with enriched Hp ^{129}Xe (85%) polarized to ~10% (Polarean, Durham NC). T_2^* values were measured for the phantom and rat lung using the FWHM of the gas and dissolved phase spectral peaks respectively. 2D axial and coronal projection spiral IDEAL Hp ^{129}Xe images were acquired with the parameters as shown in Table 1. Three echo-time shifts with a constant spacing of $\Delta TE = 50\mu\text{s}$ were selected to maximize the effective number of signal averages [3]. A non-selective RF excitation pulse was used with a width of $130\mu\text{s}$ centered on the dissolved phase of Hp ^{129}Xe , to provide minimal excitation of the gas phase. The flip angle for the dissolved and gas phase resonances were measured to be 40° and 0.5° , respectively based on free induction decays obtained following successive RF pulses.

Results: Fig. 1 shows the theoretical curves for spatial resolution (a) and SNR (b) for the spiral and Cartesian trajectory as a function of $T_{\text{readout}} / T_2^*$. The spiral approach provides an expected normalized SNR improvement factor of approximately four compared to the Cartesian IDEAL approach for $T_{\text{readout}} / T_2^*$ between 1 and 3, mainly due to the larger flip angle possible with spiral IDEAL. T_2^* blurring for both the spiral and Cartesian k-space trajectories increased with read out time and were only modestly inferior for spiral (~20%). The experimentally measured image SNR and blurring from the phantom dissolved phase image are also plotted in Fig. 1 (a) and (b), indicating good agreement with the theory. Fig. 2 shows representative axial 2D projection images of the gas (a) and dissolved phase in water (b) of the phantom, and representative coronal 2D projection images of the gas (c) and dissolved phase (d) of the healthy rat lungs, obtained using the parameters in Table 1.

	G_{max} (mT/m)	SR (T/m/s)	T_{readout} (ms)	T_2^* Gas (ms)	T_2^* Dissolved (ms)	FOV (mm)	Resolution (mm)
Phantom	210	500	14	26 ± 2	14 ± 2	70	3
<i>In vivo</i>	300	2500	4.8	9.8 ± 2	2.8 ± 1	100	5

Discussion: This study shows that the IDEAL-spiral approach is feasible for Hp ^{129}Xe imaging of the rodent lung, providing an increase in normalized SNR of a factor of approximately four for the dissolved phase. Further SNR improvements are anticipated by further shortening the read-out time through the use of interleaved spirals which will also help mitigate T_2^* blurring. These improvements are also expected to benefit imaging of dissolved ^{129}Xe in tissue and blood separately.

Acknowledgements: This work was supported by NSERC, CIHR and OPIC. O.D. was supported by a CaRTT studentship. We gratefully acknowledge Andrew Wheatley for assistance with hyperpolarized ^{129}Xe gas production. **References:** [1] A. V. Ouriadov et al., Proceedings 19th ISMRM 2011, Abstract 6040; [2] K. Qing et al., MRI 2013, 30(2): 1134–42; [3] F. Wiesinger et al., MRM 2012, 68(1):8-16; [4] H. Lee et al., MRM 2003, 50(6): 1276-85; [5] O. Doganay et al., Proceedings 21st ISMRM 2013, Abstract 1479; [6] G. W. Miller et al., MAGMA 2004, 16(5): 218–26.

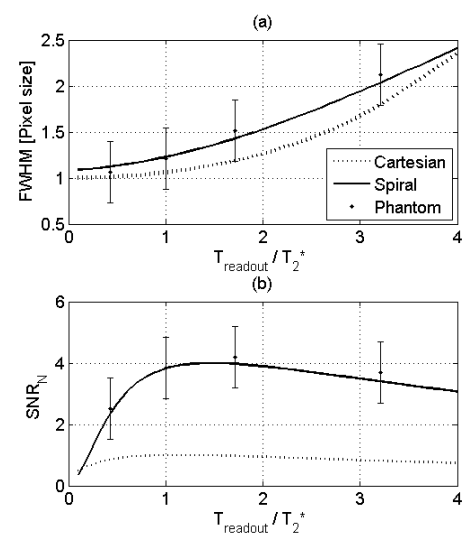


Figure 1: Theoretical spatial resolution (a) and normalized SNR_N (b) as a function of $T_{\text{readout}} / T_2^*$ for the Cartesian and spiral k-space trajectories. Phantom dissolved phase experimental results are also shown.

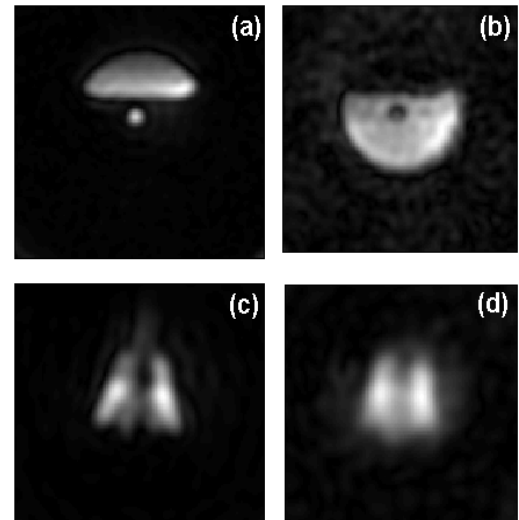


Figure 2: Representative axial gas (a) and dissolved (b) phase images of gas/dissolved Hp ^{129}Xe phantom and coronal gas (c) and dissolved (d) phase images of rat lungs.